JOURNAL OF THERMOPHYSICS AND HEAT TRANSFER
Vol. 6, No. 2, April–June 1992

Models of Energy-Exchange Mechanics Applicable to a Particle Simulation of Reactive Flow

Brian L. Haas*
Stanford University, Stanford, California 94305

Statistical particle simulations, such as the direct simulation Monte Carlo (DSMC) method, are appropriate for computationally modeling highly rarefied hypersonic flows about vehicles during atmospheric entry. Models of molecular interaction kinetics must account for the exchanges of energy occurring among the thermal energy modes during translational, rotational, and vibrational relaxation as well as dissociation, recombination, and atomic-exchange reactions in air. As presented here, models employed in a particle simulation for reaction mechanics are constrained by considerations of detailed balance at equilibrium and conservation of linear momentum and energy. Equipartition of internal energy between rotational and vibrational modes promotes equilibrium and is compatible with the quantized nature of the simple harmonic oscillator. Postreaction energies may be proportionally partitioned among the thermal energy modes contributing to reaction, followed by thermal relaxation steps to promote detailed balance at equilibrium. Reaction selection rules, as functions of reactive collision energy, are structured to yield Arrhenius reaction-rate temperature dependence at equilibrium. The models described here are verified through simulation of superheated adiabatic reservoirs relaxing thermochemically to equilibrium.

Introduction

POTENTIAL development of vehicles such as the National Aerospace Plane (NASP) and the Aero-assisted Flight Experiment (AFE) has renewed interest in modeling hypersonic rarefied flow. Such flows may be characterized by nonequilibrium between molecular energy modes and between the concentrations among different species in the rarefied gas. Temperatures exceeding 20,000 K are possible behind the leading shock of a blunt vehicle entering the atmosphere with near-orbital velocity. Such conditions excite the energy modes of diatomic molecules in air, leading to dissociation. Exchange reactions and recombination of free atoms will occur near cold catalytic surfaces and during expansion of the gas around body shoulders. The finite rates of thermal excitation and reaction processes significantly alter the character of the flowfield, affecting the temperatures, densities, and heat-transfer experienced by the vehicle. Ionization and radiation may also be significant in this flowfield but are not addressed in this work.

The degree of rarefaction of these flows, at altitudes above 80 km, is characterized by Knudsen numbers exceeding 0.01. The low-density nature of these flows is such that the familiar Navier-Stokes equations are not applicable primarily due to failure of the linear constituitive relations. By contrast, particle simulation methods are based on discrete molecular models and provide potentially powerful alternatives for simulating these flows. Considerable experience has been gained in the development[1] and application[2] of the direct simulation Monte Carlo (DSMC) method pioneered by Bird. The underlying algorithms employed in the method have been reformulated specifically for the vector- and parallel-processing architectures of modern supercomputers.[3–7] Note that comprehensive modeling of chemical kinetic processes in a gas involves solution of the Schrödinger equation, and is therefore ill-suited for large-scale simulations. However, meaningful simulations are obtained with phenomenological models, applied at the microscopic particle level, which yield the correct macroscopic thermochemical behavior.

This paper presents the fundamentals of modeling chemically reacting flows in a particle simulation with particular emphasis on reaction mechanics; a topic that has received minimal attention in the literature. The types of particles used in the simulation and their properties are presented along with a review of reaction fundamentals. Reaction selection rules, employed in the simulation, are based on reaction probabilities as functions of molecular collision energy and lead to Arrhenius temperature-dependence of the macroscopic reaction rates. Algorithms used in modeling thermal collisions are then described. Exchanges of energy involving the quantized vibrational mode are modeled in a manner employing equipartition, and do not require sampling from variable energy distributions. A convenient model, *proportional energy-partitioning*, is proposed for modeling reaction mechanics, with details of how postreaction energy is partitioned among the thermal energy modes of the products. The thermochemical models are then applied to a reservoir of superheated molecules relaxing thermally and chemically to equilibrium in order to demonstrate their ability to simulate reactive flows.

Reaction Fundamentals

Atmospheric air, under the hypersonic conditions described, can be modeled approximately by the following five-species set: O_2, N_2, NO, O, and N. A more complete model would include ions such as NO^+. Associated with each particle in the flow is its position $\boldsymbol{x} = (x, y, z)$; its velocity $\boldsymbol{u} = (u, v, w)$; its species type; and the energy of its internal modes, ϵ_{rot} and ϵ_{vib} if it is diatomic. Each species is identified by its mass, relative diameter, and characteristic temperatures of vibration and dissociation.

A given reaction may occur only if the total energy accumulated by the colliding particles, as identified below, exceeds an activation threshold E_a. Dissociation reactions proceed as indicated by the general equation

$$AB + X \rightarrow A + B + X \qquad (1)$$

Presented as Paper 90-1749 at the AIAA/ASME 5th Joint Thermophysics and Heat Transfer Conference, Seattle, WA, June 18–20, 1990; received Aug. 13, 1990; revision received March 10, 1991; accepted for publication March 17, 1991.

*Research Assistant, Department of Aeronautics and Astronautics. Student Member AIAA.

where AB is diatomic, A and B are monatomic, and X is a partner of any type. The corresponding activation threshold is given by the dissociation bond energy; that is, $E_a = D_{AB}$. This also represents the reaction energy, $\Delta E_{rxn} = D_{AB}$, which is removed from the energy modes contributing to the reaction and is stored in the electron configuration of the products.

Exchange reactions are typically of the form

$$AB + C \rightarrow AC + B \tag{2}$$

where B and C are monatomic. Collisions must have energy exceeding some threshold E_a to initiate the reaction. The reaction energy, which is removed from the thermal energy modes of the reactants and stored as potential energy in the products, is given by the difference in dissociation bond energies of the molecules involved in Eq. (2); that is, $\Delta E_{rxn} = D_{AB} - D_{AC}$.

Recombination, the reverse of dissociation, is a three-body process. Benson and Fueno[8] suggest that recombination should be modeled as a succession of binary collisions. In the first step, given by

$$A + B \rightarrow (AB) \tag{3}$$

two atoms collide and possibly form a mutually orbiting pair, denoted in parentheses as (AB). The pair remains intact for some limited lifetime depending upon the collision energy. If, during that lifetime, the orbiting pair experiences a collision with a particle of species X such that X is able to absorb some of the exothermic reaction energy, then (AB) may stabilize into molecule AB, completing the second step of recombination given by

$$(AB) + X \rightarrow AB + X \tag{4}$$

The activation threshold for recombination is simply $E_a = 0$. Upon stabilization, the reaction energy $\Delta E_{rxn} = D_{AB}$ is removed from the electron configuration of the reactants and repartitioned among the thermal energy modes of the products. If no stabilizing collision occurs, the orbital pair splits into free atoms, representing a monatomic thermal collision. Such a two-step method has been adapted for this simulation as described below.

Fundamentals of a Particle Simulation

The basic steps in a particle simulation are the collisionless motion of particles, followed by the pairing and testing of neighboring particles for possible collision. The collision selection rule employed in the present work is taken from Baganoff and McDonald,[3] and is based on the power-law intermolecular potential. Each class of interaction, involving species a and b, has associated with it a unique power-law exponent α_{ab} as used in the collision probability of the form

$$P_c \sim g^{1-4/\alpha_{ab}} \tag{5}$$

where g is the relative speed of collision. The power-law exponent typically ranges from the Maxwell-molecule limit $\alpha_{ab} = 4$ to the hard-sphere limit $\alpha_{ab} = \infty$.

Neighboring particles in the flow are paired off as potential collision candidates. For each candidate pair, a uniform random number $\Re$ is generated and compared to the collision probability P_c applicable to that pair as computed from Eq. (5). Candidate pairs are accepted as collision partners whenever $\Re < P_c$. All pairs that collide are then tested for possible reaction. Reactive collisions are processed according to the reaction mechanics models appropriate for the given reaction-type. Collisions that do not react are processed according to thermal collision mechanics, which may include an exchange of energy among the relative translational, rotational, and vibrational modes.

Contribution of Energy Modes to Reaction

As noted above, only collisions with total energy exceeding the activation threshold E_a are capable of dissociating molecule AB in the reaction of Eq. (1). That total collision energy $\epsilon_c = \Sigma\epsilon_m$, is the sum of energy from all contributing modes m and is distributed at equilibrium temperature T with ζ_c nonintegral degrees of freedom[10] in a Boltzmann distribution given by

$$f_c^*(\epsilon_c)\, d\epsilon_c = \frac{1}{\Gamma\left(\frac{\zeta_c}{2}\right)} \left(\frac{\epsilon_c}{kT}\right)^{\zeta_c/2-1} \exp\left(-\frac{\epsilon_c}{kT}\right) \frac{d\epsilon_c}{kT} \tag{6}$$

where k is Boltzmann's constant.

There has been considerable debate, however, regarding the role of internal energy modes in dissociation.[11] It is unclear which of the energy modes, present in a given collision, contribute to ϵ_c, leading to confusion over the appropriate value of ζ_c. Various theories on chemical kinetics suggest that reactions occur as a result of intimate interactions among the internal energy modes of the reactants. Sharma, Huo, and Park[12] suggest that dissociation is the result of vibration-vibration energy exchange between molecules. Here, AB acquires vibrational energy from partner X until it reaches its reaction threshold and dissociates. Hansen[13] suggests that the rotational modes contribute to vibrational excitation and possible dissociation. Such arguments imply that all modes contribute, in some way, to ϵ_c. As a practical matter, because only those collisions that satisfy the condition $\epsilon_c > D$ are dissociation candidates, it is advantageous in the simulation to include all available energy modes in the ϵ_c sum to provide a greater number of sufficiently energetic collisions from which to select reactive collisions.

This debate concerning internal energy mode contribution to reaction may be partly resolved in a self-consistent manner by consideration of detailed balance.[14] More involved reaction models, fully coupling internal modes to dissociation, have been studied extensively[12,15-17] but have yet to appear in large-scale particle simulations.

By including all available energy modes in the collision energy

$$\epsilon_c = \epsilon_{\text{rel}_{AB,X}} + \epsilon_{\text{int}_{AB}} + \epsilon_{\text{int}_X} \tag{7}$$

the number of degrees of freedom for $f_c^*(\epsilon_c)$ is simply the sum of the number of degrees of freedom from each of these statistically independent modes

$$\zeta_c = \left(4 - \frac{4}{\alpha_{AB,X}}\right)_{\text{rel}} + \zeta_{\text{int}_{AB}} + \zeta_{\text{int}_X} \tag{8}$$

In Eq. (8) the $(4 - 4/\alpha_{AB,X})$ term accounts for the relative translational energy biased[9,14] by the collision selection rule of Eq. (5). For diatomic species with rotational and vibrational internal energies, the corresponding number of internal degrees of freedom is given by

$$\zeta_{\text{int}} = 2 + \zeta_{\text{vib}} \tag{9}$$

where the vibrational mode at equilibrium has associated with it ζ_{vib} degrees of freedom, defined for the simple harmonic oscillator by[18]

$$\zeta_{\text{vib}} = \frac{2\theta_v/T}{e^{\theta_v/T} - 1} \tag{10}$$

Reaction Selection Rules

Chemistry modeling involves determining which collisions react (reaction selection) and then performing the corresponding reactions (reaction mechanics). Only a brief review

of reaction selection is provided here because the focus of the present work addresses the mechanics of thermal and reactive collisions.

Dissociation Selection

The probability P_d that a given collision between particles AB and X results in dissociation of AB as in Eq. (1) is computed as a function of the energies contributing to the collision. A uniformly generated random number $\Re$ is compared to that probability such that dissociation is accepted if $\Re < P_d$.

The expression for P_d must be determined such that the resultant forward reaction rates at equilibrium match those correlated from experiment. The rate equation defines the forward rate coefficient k_f and relates it to the dissociation probability as follows:

$$\frac{dn_{AB}}{dt} = -n_{AB}n_x k_f = -Z_{AB,X}\int_{E_a}^{\infty} P_d(\epsilon_c) f_c^*(\epsilon_c)\, d\epsilon_c \quad (11)$$

where n represents number density and $Z_{AB,X}$ is the bimolecular collision rate between particles of species AB and X. Possible forms of P_d have been suggested[13] based upon the physics of the chemical interaction kinetics. A phenomenological format adapted from Bird[19]

$$P_d \sim (\epsilon_c - E_a)^{bf-1/2+2/a}\left(1 - \frac{E_a}{\epsilon_c}\right)^{(\zeta_c/2)-1} \quad (12)$$

is structured specifically to ensure that the simulated dissociation rate, due to application of Eq. (12), matches the temperature dependence dictated by the Arrhenius expression[20] for the rate coefficient, given by

$$k_f(T) = a_f T^{bf} \exp\left(-\frac{E_a}{kT}\right) \quad (13)$$

where constants a_f, b_f, and E_a are correlated from experiment. As defined by Eqs. (8–10), ζ_c is a very *weak* function of temperature for the range of interest in hypersonic flow. We, therefore, fix ζ_c at some reference temperature T_{ref} for use in Eq. (12). Any intermediate translational temperature, taken from that portion of the flowfield dominated by reactions, is appropriate for T_{ref} because the effect of this simplification is minor and is confined to the reaction selection process. Atomic exchange reactions are also selected via Eq. (12).

Recombination Selection

As noted earlier, recombination is modeled by a two-step process. In the present work, all collisions between atoms result in the formation of orbital pairs as given by Eq. (3). Even for a highly dissociated flowfield, the concentration of (AB) remains very low. However, employing limited lifetimes to each orbital pair leads to computational complexity and inefficiency. Alternatively, in the current implementation all (AB) that collide with partners of species X during the next time step are tested for stabilization by the recombination probability function

$$P_r \sim (\epsilon_{\text{int}(AB)})^{-\phi}(\epsilon_{\text{int}X})^{-\eta} \quad (14)$$

where ϕ and η are unique positive constants per reaction, and $\epsilon_{\text{int}(AB)}$ and $\epsilon_{\text{int}X}$ are the internal energies of the orbital pair (AB) and partner X, respectively. For monatomic X, $\epsilon_{\text{int}X}$ is excluded from Eq. (14). Those collisions selected for stabilization (by comparison of a random number $\Re$ to P_r) will complete the recombination process of Eq. (4).

The equilibrium concentration coefficient K is defined for reaction (1) by

$$K = \frac{n_A n_B}{n_{AB}} \quad (15)$$

The form of P_r in Eq. (14) was chosen because it leads to the same temperature dependence of K as dictated by the Arrhenius form

$$K(T) = a_e T^{be} \exp\left(-\frac{D_{AB}}{kT}\right) \quad (16)$$

where constants a_e, b_e, and D_{AB} are correlated from experiment. The parameters in P_r, as well as the unknown interaction potential for collisions involving orbital pairs, $\alpha_{(AB),X}$ may be found in a manner similar to that employed for dissociation. However, a complete derivation involves consideration of detailed balance among the energy modes contributing to the reaction.[14]

Mechanics of Thermal Collisions

Modeling of thermal collision mechanics in the context of a particle simulation is discussed in detail by McDonald[9] and is reviewed briefly here. A collision between particles a and b has associated with it a center of mass velocity $\boldsymbol{G}$ and relative translational velocity $\boldsymbol{g} = \boldsymbol{u}_a - \boldsymbol{u}_b$. The relative translational energy ϵ_{rel} is then defined by

$$\epsilon_{\text{rel}} = 1/2\ \mu_{ab} g^2 \quad (17)$$

where $\mu_{ab} = m_a m_b/(m_a + m_b)$ is the reduced mass of the pair. Neglecting the electronic modes, the energies available in a given collision include ϵ_{rel} and the rotational and vibrational internal energies of a and b.

Mechanics of Elastic Collisions

After an elastic collision, the particles separate with relative translational velocity $\boldsymbol{g}'$, which is simply a random reorientation of the collision approach velocity $\boldsymbol{g}$. This represents spherically uniform scattering of postcollision velocities adapted from the Variable Hard-Sphere (VHS) model of Bird.[21] There is no alteration of the internal modes of either particle. Note the use of superscript $'$ to denote postcollision quantities.

Mechanics of Rotational Relaxation

Some collisions may lead to an exchange of energy between the translational mode and one or both of the internal energy modes, promoting relaxation of the gas toward thermal equilibrium. Those collisions relaxing the rotational mode are generally more frequent than those relaxing the vibrational mode.

Rotationally relaxing thermal collisions involve repartitioning of the combined energy $\epsilon_{\text{rel}} + \epsilon_{\text{rot}}$ among the relative translational and rotational modes of the collision. The method of Borgnakke and Larsen[22] is employed here by sampling the fraction

$$F = \frac{\epsilon_{\text{rot}}}{\epsilon_{\text{rel}} + \epsilon_{\text{rot}}} \quad (18)$$

directly from its equilibrium distribution $f^*(F)$. Because $f^*(F)$ is dependent only upon the intermolecular potential parameter $\alpha_{a,b}$, it is unique for each pair of species $a + b$ and is invariant with temperature when assuming that the translational and rotational energy distributions are continuous.[9] The postcollision energies are then given by

$$\begin{aligned} \epsilon'_{\text{rot}} &= (\epsilon_{\text{rel}} + \epsilon_{\text{rot}})F \\ \epsilon'_{\text{rel}} &= (\epsilon_{\text{rel}} + \epsilon_{\text{rot}}) - \epsilon'_{\text{rot}} \end{aligned} \quad (19)$$

If both particles in the collision are diatomic, then ϵ'_{rot} is randomly divided between their respective rotational modes to promote equilibrium. A probability P_{rot} is used to select which collisions promote rotational relaxation.

Mechanics of Vibrational Relaxation

Collisions that promote vibrational relaxation, selected with probability P_{vib}, are not well suited to the Borgnakke-Larsen model employed in rotational relaxation. Attempts to do so are afforded by approximating the discrete distribution of vibrational energy at equilibrium by a continuous Boltzmann distribution with ζ_{vib} degrees of freedom. Unfortunately, ζ_{vib} varies with temperature as does the resulting distribution $f^*(F)$. As such, a new distribution must be sampled for each colliding pair depending upon some local temperature that is ill-defined for a flow in thermal nonequilibrium. Alternatively, McDonald[9] models vibrational relaxation in a manner that avoids direct sampling from equilibrium distributions such as $f^*(F)$. That model will be adapted here to facilitate its use in reaction mechanics, and is based on the following efficient iteration scheme. First, energy is exchanged between rotation and vibration, followed by an exchange between rotation and translation via rotational-relaxation as outlined above. These steps may then be repeated, iterating toward equilibrium.

Note that consideration must be made of the quantum nature of the vibrational mode. For the simple harmonic oscillator, we define vibrational energy, measured relative to the ground state, $\frac{1}{2}k\theta_v$, by

$$\epsilon_{\text{vib}} = q_{\text{vib}}(k\theta_v) \tag{20}$$

where q_{vib} represents the number of quanta associated with a given vibrator, and $k\theta_v$ represents the characteristic vibrational energy per quantum level.

To model the random mixing of rotational and vibrational energies of a given particle in a manner that promotes equilibrium, we take advantage of *equipartition*, the fundamental physical assumption of statistical mechanics.[18] This postulates that all possible divisions of internal energy

$$\epsilon_{\text{int}} = \epsilon_{\text{rot}} + \epsilon_{\text{vib}} \tag{21}$$

among the internal modes, ϵ'_{rot} and ϵ'_{vib}, are *equally probable*.

First, ϵ_{int} is quantized by the characteristic vibrational energy $k\theta_v$ resulting in $Q + 1$ quantum levels: $0, 1, \ldots, Q$. The limit Q is found from

$$Q = \left[\frac{\epsilon_{\text{int}}}{k\theta_v}\right] \tag{22}$$

where the brackets [ ] denote truncation.

Upon division, the outcome quantum level for vibration q'_{vib} must be equally likely among these $Q + 1$ quantum levels. This is achieved by simply generating a floating-point random number in the range $[0, Q + 1)$, and truncating to the nearest level, as given by

$$q'_{\text{vib}} = [\mathcal{R}(Q + 1)] \tag{23}$$

where $\mathcal{R}$ is a uniformly generated random number in the range $[0, 1)$. From Eq. (23), the postcollision internal energies of the particle are given by

$$\epsilon'_{\text{vib}} = q'_{\text{vib}}(k\theta_v) \tag{24}$$

$$\epsilon'_{\text{rot}} = \epsilon_{\text{int}} - \epsilon'_{\text{vib}} \tag{25}$$

As proven in the Appendix to this article, applying this method of energy partition among the internal modes of a diatomic molecule will satisfy detailed balance between the vibrational and rotational modes at equilibrium. When out of equilibrium, however, this exchange must be augmented by rotational-relaxation steps in Eqs. (18) and (19) to relax fully the rotational mode.

Mechanics of Reactive Collisions

Once reactive collisions have been identified from the reaction selection rules of Eqs. (12) and (14), the mechanics of those reactions must be performed. All reactions of interest in hypersonics involve some alteration of the energy modes contributing to the reaction. The objective here is to determine how to account for reaction energy ΔE_{rxn} by altering each of the thermal energy modes involved in the reaction just prior to splitting or joining particles into products. The chemical-kinetic details are not well understood regarding energy partition among the energy modes of particles during reaction. However, the modeling of reaction mechanics must adhere to certain fundamental constraints, including detailed balance at equilibrium and conservation of momentum and energy.

Proportional Energy-Partitioning Model

Recall the energies of Eq. (7) contributing to the dissociative collision of Eq. (1). During reaction, the dissociation energy must be removed from the collision energy

$$\epsilon''_c = \epsilon_c - \Delta E_{\text{rxn}} \tag{26}$$

$$= \epsilon_{\text{rel}AB,X} + \epsilon_{\text{rot}AB} + \epsilon_{\text{vib}AB} + \epsilon_{\text{int}X} - \Delta E_{\text{rxn}} \tag{27}$$

$$= \epsilon''_{\text{rel}AB,X} + \epsilon''_{\text{rot}AB} + \epsilon''_{\text{vib}AB} + \epsilon''_{\text{int}X} \tag{28}$$

Note the use of superscript " to denote postreaction quantities.

Though it is unclear how to redistribute the energies of Eq. (27) among those of Eq. (28), a convenient means to account for the alteration of each energy mode m is to remove *proportionally* the reaction energy ΔE_{rxn} from each mode, resulting in postdissociation energies ϵ''_m given by

$$\epsilon''_m = \epsilon_m - \frac{\epsilon_m}{\epsilon_c}\Delta E_{\text{rxn}} = \epsilon_m\left(1 - \frac{\Delta E_{\text{rxn}}}{\epsilon_c}\right) \tag{29}$$

This method is simple to implement and can be applied to exchange reactions and recombination as well. Note, however, that in exothermic reactions, ΔE_{rxn} will be proportionally added to each contributing energy mode rather than removed.

At equilibrium, detailed balance dictates that there exists no net energy transfer among energy modes of all species in the gas. As a consequence, the reaction models must promote, or relax to, equilibrium for a gas in thermochemical nonequilibrium. If a relaxing ensemble of particles reaches steady state, yet exhibits nonequilibrium behavior such as a difference in mode temperatures, then the reaction model is in error.

Similar to the method of Borgnakke and Larsen employed in rotational relaxation above, partitioning postreaction energies among the energy modes by sampling directly from equilibrium distributions would promote relaxation toward equilibrium for reactive collisions. Doing so, however, requires that these distributions be available at all temperatures and for all possible reactions. This leads to difficulties similar to those encountered in modeling vibrational relaxation. Alternatively, the proportional energy-partitioning model above avoids this difficulty because it requires no access to equilibrium distributions, but falters in that it will not readily promote equilibrium for a flow initially in thermal nonequilibrium. This is remedied by adding the thermal relaxation steps of Eqs. (18–25) to this algorithm for reaction mechanics.

Mechanics of Dissociation

Simulation of dissociation reaction (1) may be divided into two steps. First, the dissociation energy is removed from the reactants, creating temporary products, as described by

$$AB + X \rightarrow AB'' + X'' \tag{30}$$

The products AB'' and X'' separate with relative translational energy $\epsilon''_{\text{rel}_{AB,X}}$ modified according to the proportional energy-exchange model of Eq. (29). As mentioned earlier, decomposing a relative energy into postcollision velocities involves random reorientation of the postreaction relative velocity vector $\mathbf{g}''_{AB,X}$ as found from $\epsilon''_{\text{rel}_{AB,X}}$ and Eq. (17).

If X is diatomic, the postdissociation states of its internal energies are not found individually by application of Eq. (29), because consideration must be made of the quantum nature of the vibrational mode. Rather, the internal energy as a whole is depleted according to Eq. (29)

$$\epsilon''_{\text{int}X} = \epsilon_{\text{int}X}\left(1 - \frac{\Delta E_{\text{rxn}}}{\epsilon_c}\right) \tag{31}$$

and is then redistributed between $\epsilon''_{\text{rot}X}$ and $\epsilon''_{\text{vib}X}$ according to the steps employed for vibrational relaxation in Eqs. (22–25). If X is monatomic, $\epsilon_{\text{int}X}$ will remain zero.

Now that AB'' and X'' have separated, the second step in the dissociation reaction involves splitting AB'' into free atoms, given by

$$AB'' \rightarrow A + B \tag{32}$$

To conserve linear momentum and energy, all of the postdissociation internal energy of AB'' must be converted into relative translational energy for the separation of A and B

$$\epsilon_{\text{rel}A,B} = \epsilon''_{\text{int}AB} = (\epsilon_{\text{rot}AB} + \epsilon_{\text{vib}AB})\left(1 - \frac{\Delta E_{\text{rxn}}}{\epsilon_c}\right) \tag{33}$$

The mechanics for exchange reactions from Eq. (2) are identical to those for dissociation.

Mechanics of Orbital Pair Formation

Orbital pair formation is the first step in recombination modeling as given by Eq. (3), where two atoms A and B join to form a single temporary orbital pair (AB). Conservation of linear momentum dictates that the velocity of (AB) must be the same as the center of mass velocity of the $A + B$ collision $G_{A,B}$. Conservation of energy requires that the relative translational energy $\epsilon_{\text{rel}A,B}$ must be stored internally in (AB):

$$\epsilon_{\text{int}(AB)} = \epsilon_{\text{rel}A,B} \tag{34}$$

If (AB) remains uncollided on the next time step, it is split into free atoms A and B. Doing so simply requires that $\epsilon_{\text{int}(AB)}$ be converted back into $\epsilon_{\text{rel}A,B}$.

Mechanics of Orbital Pair Stabilization

Orbital pair stabilization, given by Eq. (4), represents the second step that completes the recombination reaction. The reaction energy $\Delta E_{\text{rxn}} = D_{AB}$ must be absorbed by the thermal energy modes of the products, such that the postreaction collision energy is given by

$$\begin{aligned}\epsilon''_c &= \epsilon_{\text{rel}(AB),X} + \epsilon_{\text{int}(AB)} + \epsilon_{\text{int}X} + \Delta E_{\text{rxn}} \\ &= \epsilon''_{\text{rel}(AB),X} + \epsilon''_{\text{int}(AB)} + \epsilon''_{\text{int}X} \\ &= \epsilon_{\text{rel}AB,X} + \epsilon_{\text{int}AB} + \epsilon''_{\text{int}X}\end{aligned} \tag{35}$$

According to the proportional energy-partitioning concept, the relative translational energy of separation of stabilized molecule AB and collision partner X is found by adapting Eq. (29)

$$\epsilon_{\text{rel}AB,X} = \epsilon''_{\text{rel}(AB),X} = \epsilon_{\text{rel}(AB),X}\left(1 + \frac{\Delta E_{\text{rxn}}}{\epsilon_c}\right) \tag{36}$$

The internal energies of X, if applicable, are found in the same way as in dissociation from Eq. (31), with the exception that reaction energy is added rather than removed.

Likewise, the internal energy of AB, given by

$$\epsilon_{\text{int}AB} = \epsilon''_{\text{int}(AB)} = \epsilon_{\text{int}(AB)}\left(1 + \frac{\Delta E_{\text{rxn}}}{\epsilon_c}\right) \tag{37}$$

is distributed among its rotational and vibrational modes according to the method employed for vibrational relaxation in Eqs. (22–25). However, as stated earlier and as proven in the appendix, these steps must be augmented by rotational relaxation to promote equilibrium distributions for a gas initially out of equilibrium.

Reservoir Simulation and Results

A single-species, adiabatic reservoir of molecules, superheated in translation and rotation to temperature T_o, will relax to thermochemical equilibrium through reactions and energy-mode exchanges. The final temperature T^* and composition can be determined analytically.[23] The relaxation history of this reservoir is similar to that behind a normal shock wave. The reservoir is simulated during thermal relaxation both with and without chemical relaxation.

In the external flows typically associated with hypersonic re-entry vehicles, dissociation and exchange reactions dominate the flowfield chemistry. However, the objective here is to test the simulation in an environment in which *all* types of chemical reactions (dissociation, exchange, and recombination) are pronounced, such as would occur at equilibrium if the temperature and diatomic concentrations remained high. Consequently, to simulate thermochemical relaxation to equilibrium, a model species A_2 is used which is similar to O_2 except that a_e is altered, effectively increasing the recombination rate, allowing greater concentration of diatomic particles at high equilibrium temperature where reactions are significant. Such a gas represents a "worst-case scenario" in which recombination has pronounced effects to better demonstrate the capability of the reaction models. Table 1 lists the properties associated with this model gas. The reactions pertaining to A_2 are

$$A_2 + A_2 \rightleftharpoons A + A + A_2 \tag{38}$$

$$A_2 + A \rightleftharpoons A + A + A \tag{39}$$

Thermal Relaxation Results

Thermally relaxing collisions, as modeled in Eqs. (18–25), will excite the vibrational mode of molecules in the reservoir leading to an increase in the vibrational temperature accompanied by a decrease in the translational and rotational temperatures. The temperature for each energy mode is plotted in Fig. 1 during simulated thermal relaxation from T_o = 24,452 K to steady state. The rates of internal mode relaxation were controlled by invariant probabilities $P_{\text{rot}} = 0.20$ and $P_{\text{vib}} = 0.02$, adapted from Bird.[23] Energy-dependent forms of these probabilities, suggested by Boyd[24,25] and Haas,[14] would better model thermal relaxation in the transient portion of the flow, but are of little benefit here in studying equilibrium behavior.

Table 1 Properties[2,18,20] of model gas A_2 and A

Characteristic vibrational temp.	θ_v = 2270 K
Dissociation threshold	D/k = 59,400 K
Forward rate coefficient, m³/(molecule − s)	
$A_2 + A_2$:	$k_f = 4.58 \times 10^{-11} T^{-1.00} e^{-D/kT}$
$A_2 + A$:	$k_f = 1.37 \times 10^{-10} T^{-1.00} e^{-D/kT}$
Concentration coefficient, mole/cm³	
	$K = 0.40\ T^{-0.5} e^{-D/kT}$

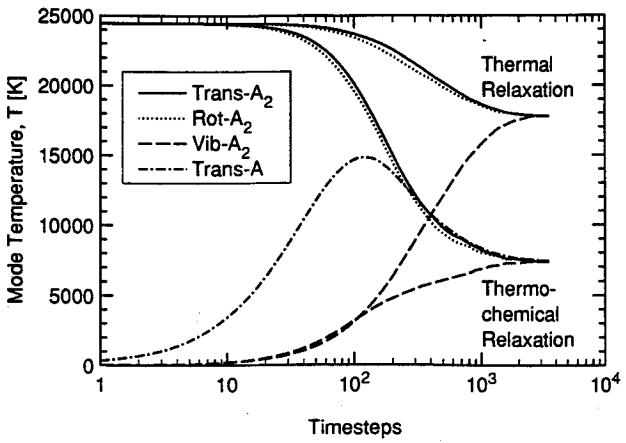

Fig. 1 Temperature per mode in thermal relaxation to steady-state of a simulated reservoir with and without chemical reactions. The diatomic gas, for which θ_v = 2270 K, is initialized with no vibrational energy and $T_{trans} = T_{rot}$ = 24,452 K.

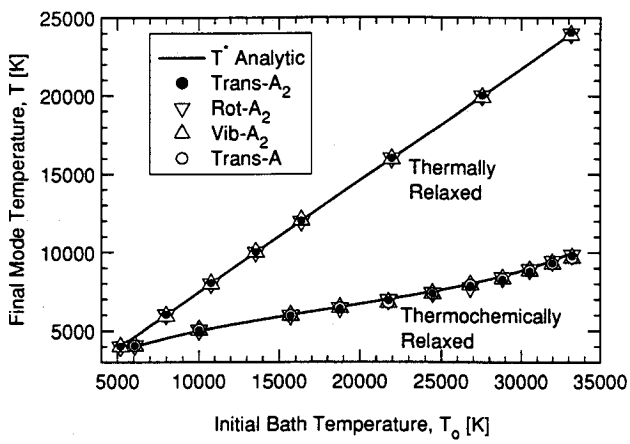

Fig. 2 Steady-state temperature per energy mode compared to the analytic equilibrium temperature T^* in simulated thermal relaxation and thermochemical relaxation of a gas reservoir.

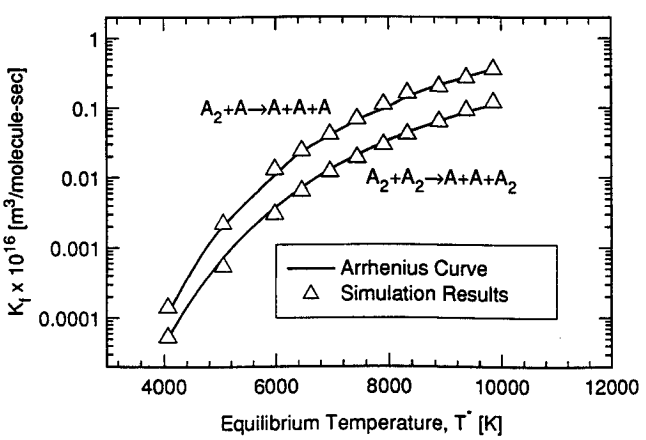

Fig. 3 Forward reaction rate k_f at steady-state vs equilibrium temperature compared with Arrhenius fit in A_2 relaxation simulations.

The simulation is repeated for several values of T_o over a large temperature-range. The analytic curve for equilibrium temperature T^* as well as the steady-state temperature per energy mode is plotted against T_o in Fig. 2. Convergence of all mode temperatures to the corresponding analytic values demonstrates the ability of the models to promote thermal relaxation to equilibrium.

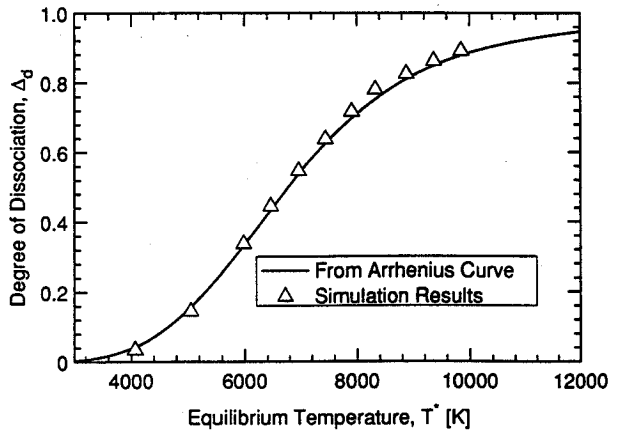

Fig. 4 Degree of dissociation Δ_d at steady-state vs equilibrium temperature compared with Arrhenius fit in A_2 relaxation simulations.

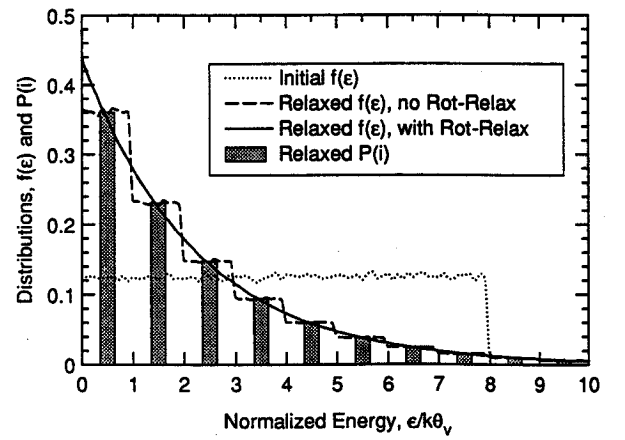

Fig. 5 Discrete and continuous energy distributions in a diatomic reservoir at steady-state after thermal relaxation via mixing algorithm from Eqs. (22–25), with and without rotational relaxation steps. The reservoir was initialized with no discrete vibrational energy and uniformly distributed continuous rotational energy.

Thermochemical Relaxation Results

Also plotted in Fig. 1 is the thermochemical relaxation of A_2 to steady state. The mode temperatures corresponding to translation, rotation, and vibration are individually plotted in time as they converge to the equilibrium temperature T^* = 7500 K. The simulation was initialized with 40,000 diatomic particles and ran for 2500 transient steps and 1000 steady-state sampling steps.

The relaxation simulation was then repeated for equilibrium temperatures in the range 4000 K < T^* < 10,000 K, with reference temperature T_{ref} = 7000 K. For each case, the resulting equilibrium temperature per mode reached by the simulation is compared to the analytic value in Fig. 2. The close agreement between mode temperatures indicates that detailed balance is maintained, as is necessary for equilibrium. The simulated forward rate coefficient per reaction is plotted against T^* in Fig. 3, and is compared to the Arrhenius curve of $k_f(T^*)$. Likewise, Fig. 4 compares the degree of dissociation Δ_d for these runs against the Arrhenius fit, where Δ_d is defined as follows

$$\Delta_d \equiv \frac{n_A}{2n_{A_2} + n_4} \tag{40}$$

and is related to the equilibrium concentration coefficient as follows

$$K = 2(2n_{A_2} + n_A)\frac{\Delta_d^2}{1 - \Delta_d} \tag{41}$$

These plots indicate that the simulation does capture the correct equilibrium behavior of a relaxing gas as predicted by the experimental Arrhenius correlations of reaction rates and species concentrations over a large temperature range.

Concluding Remarks

No direct attempt was made here to model the transient of the relaxing bath; comparisons to known behavior were only made at equilibrium. However, the chemistry models are based on principles of molecular interaction, independent of the equilibrium assumption used only to evaluate reaction selection parameters.

The reaction selection rules, reviewed here, reproduce the Arrhenius forward reaction rates and species concentrations as correlated from experiment at equilibrium. Likewise, the individual energy mode temperatures during simulated thermal and thermochemical relaxation of nonequilibrium reservoirs converged upon the correct equilibrium values, verifying the models for collision/reaction mechanics. These models, based on proportional partitioning of postreaction energies among the contributing energy modes, conveniently account for reaction energies in a manner consistent with the constraints of detailed balance and conservation of linear momentum and energy. However, essential to these routines is the inclusion of thermal-relaxation steps, which promote thermal equilibrium during reaction and are compatible with the quantum nature of the vibrational energy mode.

Appendix: Proof of Equilibrium Convergence

The algorithm described by Eqs. (22–25) for redistributing internal energy represents random mixing of continuous and discrete distributions pertaining to the rotational and vibrational energy modes, respectively. The objective here is to prove that this algorithm promotes equilibrium.

The equilibrium distribution of rotational energy, for which $\zeta_{rot} = 2$, can be rewritten from Eq. (6) in the form

$$f^*(\varepsilon) = e^{-\varepsilon}\,d\varepsilon \tag{A1}$$

where $\varepsilon = \epsilon_{rot}/kT$ is normalized energy, and superscript * denotes equilibrium. Quantizing this distribution with respect to the normalized characteristic energy of vibration $\bar{\varepsilon} = k\theta_v/kT$ results in the discrete equilibrium distribution over vibrational quantum levels i

$$\begin{aligned} P^*(i) &= \int_{i\bar{\varepsilon}}^{(i+1)\bar{\varepsilon}} f^*(\varepsilon)\,d\varepsilon \\ &= \omega^i(1-\omega) \end{aligned} \tag{A2}$$

where $\omega = e^{-\bar{\varepsilon}} \le 1$ is a convenient grouping of terms. For a given rotational energy ε we associate a quantum value $j = \lfloor \varepsilon/\bar{\varepsilon} \rfloor$, which is also distributed as in Eq. (A2), such that the total quanta from Eq. (22) is $Q = i + j$. The normalized surplus energy remaining after truncation is defined by

$$\xi = \varepsilon - j\bar{\varepsilon} \tag{A3}$$

and is distributed according to $f^*(\varepsilon)$ upon renormalizing over the quantum level j for which $d\xi = d\varepsilon$

$$\begin{aligned} f_\xi^*(\xi)\,d\xi &= \frac{f^*(\varepsilon)\,d\varepsilon}{\int_{j\bar{\varepsilon}}^{(j+1)\bar{\varepsilon}} f^*(\varepsilon)\,d\varepsilon} \\ &= \frac{e^{-(j\bar{\varepsilon}+\xi)}\,d\xi}{e^{-j\bar{\varepsilon}}(1-e^{-\bar{\varepsilon}})} \\ &= \frac{e^{-\xi}}{(1-\omega)}\,d\xi \end{aligned} \tag{A4}$$

Note that $f_\xi^*(\xi)$ is independent of rotational quantum level j.

Baganoff[26] arrived at the outcome distributions $P(i')$ and $P(j')$ in the following manner. Let i' and j' denote the outcome quantum levels due to uniform, random division of total quanta Q. The *conditional* distribution for i', given Q, is therefore constant over the $Q + 1$ possible outcomes

$$P(i'|Q) = \frac{1}{Q+1} \tag{A5}$$

The *joint* distribution of i' and Q is then

$$P(i', Q) = P(i'|Q)P_Q^*(Q) \tag{A6}$$

where the distribution of Q is given by

$$\begin{aligned} P_Q^*(Q) &= P^*(0)P^*(Q) + P^*(1)P^*(Q-1) + \cdots \\ &= \sum_{i=0}^{Q} P^*(i)P^*(Q-i) \end{aligned} \tag{A7}$$

The resulting distribution over i' is found by summing Eq. (A6) over all Q

$$\begin{aligned} P(i') &= \sum_{Q=i'}^{\infty}\sum_{i=0}^{Q} P^*(i)P^*(Q-i)P(i'|Q) \\ &= \sum_{Q=i'}^{\infty}\sum_{i=0}^{Q} \frac{(1-\omega)^2\omega^Q}{Q+1} \\ &= (1-\omega)^2 \sum_{Q=i'}^{\infty} \omega^Q \\ &= (1-\omega)^2\omega^{i'} \sum_{k=0}^{\infty} \omega^k \\ &= \omega^{i'}(1-\omega) \end{aligned} \tag{A8}$$

Comparison of Eq. (A8) to Eq. (A2) proves that the algorithm maintains the *discrete* equilibrium distributions for vibration and rotation.

The rotational energy after mixing is

$$\varepsilon' = j'\bar{\varepsilon} + \xi \tag{A9}$$

where $j' = Q - i'$, such that $d\varepsilon' = d\xi$ over the quantum interval j'. The conditional distribution of outcomes for ε' is simply the joint distribution of j' and ξ, given Q, found by multiplying Eqs. (A4) and (A5)

$$\begin{aligned} f(\varepsilon'|Q)\,d\varepsilon' &= P(j'|Q)f_\xi^*(\xi)\,d\xi \\ &= \frac{e^{-\xi}\,d\xi}{(Q+1)(1-\omega)} \end{aligned} \tag{A10}$$

Following the same development as in (A8), we solve for the distribution over ε' by summing the joint distribution over all Q

$$\begin{aligned} f(\varepsilon')\,d\varepsilon' &= \sum_{Q=j'}^{\infty}\sum_{j=0}^{Q} P^*(j)P^*(Q-j)f(\varepsilon'|Q)\,d\varepsilon' \\ &= \sum_{Q=j'}^{\infty}\sum_{j=0}^{Q} \frac{(1-\omega)\omega^Q e^{-\xi}\,d\xi}{Q+1} \\ &= (1-\omega)e^{-\xi}\,d\xi \sum_{Q=j'}^{\infty} \omega^Q \\ &= (1-\omega)e^{-\xi}\omega^{j'}\,d\xi \sum_{k=0}^{\infty} \omega^k \\ &= (1-\omega)e^{-\xi}e^{-j'\bar{\varepsilon}} \frac{1}{(1-\omega)}\,d\xi \\ &= e^{-(j'\bar{\varepsilon}+\xi)}\,d\xi \\ &= e^{-\varepsilon'}\,d\varepsilon' \end{aligned} \tag{A11}$$

Equations (A8) and (A11) prove that the mixing algorithm maintains both the discrete and continuous distributions at equilibrium.

It can be shown that Eq. (A8), when based upon nonequilibrium distributions, leads to rate equations for the distribution functions $P(i')$ and $P(j')$. Making extensive use of generating functions, exact solutions of these rate equations are found[26] to yield exponential relaxation to discrete Boltzmann distributions $P^*(i')$ and $P^*(j')$. However, the continuous distribution $f(\varepsilon')$ will only reach equilibrium if both $P(j')$ and $f_\xi(\xi)$ equilibrate. Unfortunately, the distribution over ξ experiences no mixing in this algorithm and, therefore, will not relax toward equilibrium unless additional rotational relaxation steps are included.

To test the algorithm, an adiabatic reservoir was initialized with no vibrational energy and with rotational energy uniformly distributed, and was then thermally relaxed via the mixing algorithm described here. Two test-cases were run, one which included the rotational relaxation steps, and one which did not. The initial and final distributions for rotation are shown in Fig. 5, along with the final distribution for vibration. Note that both the discrete and the continuous distributions are of Boltzmann form for the algorithm that included rotational relaxation. However, when rotational relaxation was excluded, the continuous distribution within each quantum interval did not relax, but remained uniformly distributed. These tests prove that, for a gas out of equilibrium, the mixing algorithm will relax the discrete distributions to equilibrium, but additional rotational-relaxation is needed to achieve equilibrium for the continuous distribution.

Acknowledgments

The author acknowledges and appreciates the guidance of D. Baganoff and the assistance of M. Sussman, J. D. McDonald, and I. D. Boyd. Also acknowledged is the support of the NASA Ames Research Center for use of their facilities. This work was sponsored by Air Force Office of Scientific Research Grant AFOSR 88-0139 and NASA Grant NAGW-965.

References

[1]Bird, G. A., *Molecular Gas Dynamics*, Clarendon Press, Oxford, England, UK, 1976.

[2]Celenligil, M. C., Bird, G. A., and Moss, J. N., "Direct Simulation of Three-Dimensional Hypersonic Flow About Intersecting Wedges," *AIAA Journal*, Vol. 27, No. 11, 1989, pp. 1536–1542.

[3]Baganoff, D., and McDonald, J. D., "A Collision-Selection Rule for a Particle Simulation Method Suited to Vector Computers," *Physics of Fluids A: Fluid Dynamics*, Vol. 2, No. 7, 1990, pp. 1248–1259.

[4]Boyd, I. D., "Vectorization of a Monte Carlo Simulation Scheme for Nonequilibrium Gas Dynamics," *Journal of Computational Physics*, Vol. 96, No. 2, pp. 411–427, 1991.

[5]Dagum, L., "On The Suitability of the Connection Machine for Direct Particle Simulation," Ph.D. Thesis, Dept. of Aeronautics and Astronautics, Stanford Univ., Stanford, CA, 1990.

[6]Wilmoth, R., "Application of a Parallel DSMC Method to Hypersonic Rarefied Flows," AIAA Paper 91-0772, Reno, NV, 1991.

[7]McDonald, J. D., "Particle Simulation in a Multiprocessor Environment," AIAA Paper 91-1366, Honolulu, Hawaii, 1991.

[8]Benson, S. W., and Fueno, T., "Mechanism of Atom Recombination by Consecutive Vibrational Deactivations," *Journal of Chemical Physics*, Vol. 36, No. 6, 1962, pp. 1597–1607.

[9]McDonald, J. D., "A Computationally Efficient Particle Simulation Method Suited to Vector Computer Architectures," Ph.D. Thesis, Dept. of Aeronautics and Astronautics, Stanford University, Stanford, CA, 1990.

[10]Hinshelwood, C. N., *The Kinetics of Chemical Change*, Clarendon Press, Oxford, England, UK, 1940.

[11]Clarke, J. F., and McChesney, M., *Dynamics of Relaxing Gases*, 2nd ed., Butterworth, Stoneham, MA, 1976.

[12]Sharma, S. P., Huo, W. M., and Park, C., "The Rate Parameters For Coupled Vibration-Dissociation In A Generalized SSH Approximation," AIAA Paper 88-2714, San Antonio, TX, 1988.

[13]Hansen, C. F., "Rate Processes in Gas Phase," NASA Reference Publication 1090, 1983.

[14]Haas, B. L., "Thermochemistry Models Applicable to a Vectorized Particle Simulation," Ph.D. Thesis, Dept. of Aeronautics and Astronautics, Stanford Univ., Stanford, CA, 1990.

[15]Boyd, I. D., "Assessment of Chemical Nonequilibrium in Rarefied Hypersonic Flow," AIAA Paper 90-0145, Reno, NV, 1990.

[16]Landrum, D. B., and Candler, G. V., "Vibration-Dissociation Coupling in Nonequilibrium Flows," AIAA Paper 91-0466, Reno, NV, 1991.

[17]Haas, B. L., and Boyd, I. D., "Models for Vibrationally-Favored Dissociation Applicable to a Particle Simulation," AIAA Paper 91-0774, Reno, NV, 1991.

[18]Vincenti, W. G., and Kruger, C. H., *Introduction to Physical Gas Dynamics*, Wiley, New York, 1965.

[19]Bird, G. A., "Simulation of Multi-Dimensional and Chemically Reacting Flows," *Rarefied Gas Dynamics*, the 11th International Symposium on Rarefied Gas Dynamics, Cannes, France, July 1978 (1979).

[20]Bortner, M. H., "A Review of Rate Constants of Selected Reactions of Interest in Re-Entry Flow Fields in the Atmosphere," National Bureau of Standards Technical Note 484, 1969.

[21]Bird, G. A., "Monte-Carlo Simulation In An Engineering Context," *Rarefied Gas Dynamics*, Paper 221 of the 12th International Symposium on Rarefied Gas Dynamics, Charlottesville, VA, July, 1980.

[22]Borgnakke, C., and Larsen, P. S., "Statistical Collision Model for Monte Carlo Simulation of Polyatomic Gas Mixture," *Journal of Computational Physics*, Vol. 18, 1975, pp. 405–420.

[23]Bird, G. A., "Direct Molecular Simulation of a Dissociating Gas," *Journal of Computational Physics*, Vol. 25, 1977, pp. 353–365.

[24]Boyd, I. D., "Rotational-Translational Energy Transfer In Rarefied Nonequilibrium Flows," *Physics of Fluids A: Fluid Dynamics*, Vol. 2, No. 3, 1990, pp. 447–452.

[25]Boyd, I. D., "Analysis of Vibrational-Translational Energy Transfer Using the Direct Simulation Monte Carlo Method," *Physics of Fluids A: Fluid Dynamics*, Vol. 3, No. 7, pp. 1785–1791, 1990

[26]Baganoff, D., Private communication, 1988.